THE ASTROPHYSICAL JOURNAL, 454:L61–L64, 1995 November 20

SIMULTANEOUS OBSERVATION OF DIRECT AND RAMAN-SCATTERED O VI LINES IN THE SYMBIOTIC NOVA RR TELESCOPII[1]

BRIAN R. ESPEY,[2] REGINA E. SCHULTE-LADBECK,[3] GERARD A. KRISS,[2] FRED HAMANN,[4] HANS M. SCHMID,[5] AND JONI J. JOHNSON[6]
Received 1995 July 5; accepted 1995 September 6

ABSTRACT

The optical spectra of some symbiotic binaries show two lines in the red region of the spectrum that cannot be identified with any known allowed or forbidden transitions. A case has been made that these lines are Raman-scattered O VI λλ1032, 1038 emission lines. We present simultaneous far-UV and optical spectra of the symbiotic nova RR Tel, obtained with the Hopkins Ultraviolet Telescope and the Anglo-Australian Telescope during the Astro-2 Space Shuttle mission. These data show the first coincident detection of the strong O VI λλ1032, 1038 doublet and λλ6825, 7082 emission lines. The latter display strong linear polarization and provide new information on the structure of the nebular material. Our observations provide strong evidence for the Raman effect in RR Tel.

Subject headings: atomic processes — binaries: symbiotic — stars: individual (RR Telescopii) — ultraviolet: stars

1. INTRODUCTION

Roughly half the symbiotic stars so far surveyed show two strong, broad (FWHM ≈ 20 Å, or ∼860 km s^{-1}) emission lines at 6825 and 7082 Å. The lines are especially seen in systems that show high excitation features, and often the λ6825 feature ranks among the 10 strongest optical lines of a symbiotic star's spectrum (Allen 1980). For many years the identification of these features was uncertain, and they simply became known as the "unidentified" lines. Schmid (1989) proposed an identification of the λλ6825, 7082 lines as Raman-scattered O VI λλ1032, 1038 resonance lines. In the Raman process, inelastic scattering occurs when an O VI photon excites atomic hydrogen from its ground state to a virtual state intermediate between the $n = 2$ and $n = 3$ levels, followed by the emission of a photon, which leaves the atom in the $2s^2$ S-state. The frequency of the scattered photon is determined by the difference between the energy of the virtual and the final states of the atom, i.e., $\lambda_{\rm O\ VI}^{-1} - \lambda_{\rm Ly\alpha}^{-1} = \lambda_{\rm Raman}^{-1}$. Because of this relationship, the width of the ultraviolet O VI doublet lines is stretched by ∼6.7 times, the result being a pair of broad polarized lines in the red region of the spectrum (Nussbaumer, Schmid, & Vogel 1989).

Circumstantial evidence for the occurrence of the Raman effect in symbiotic stars in general, and for RR Tel in particular, comes from a variety of observations. Because of the small cross section for Raman scattering, the main prerequisite for this process is strong O VI emission (Nussbaumer et al. 1989). Indirect evidence for the driving O VI λλ1032, 1038 lines has come from a number of sources. Among these are the presence of O V λ1371 emission that arises, at least in part, from dielectronic recombination from O^{5+} (Hayes & Nussbaumer 1986) and the presence of Fe II transitions that are excited by O VI photons (Johansson 1988; Feibelman, Bruhweiler, & Johansson 1991). The *Voyager* spacecraft observed a number of symbiotic stars, including RR Tel, in the far-UV region of the spectrum and found evidence for strong emission in the Lyβ/O VI region of the spectrum, but because of the low resolution of these detectors (∼20 Å for a point source), the exact amount of O VI and Lyβ emission was not clear. More recently, observations made with *ORFEUS* during a Space Shuttle mission in 1993 September have revealed unambiguous detections of O VI in a number of symbiotic stars, including RR Tel, at a resolution of 0.3 Å (J. Krautter 1995, private communication).

Schmid & Schild (1990) first proposed that the λλ6825, 7082 lines should be polarized because of the dipole nature of Raman scattering. They subsequently conducted the first spectropolarimetric survey of these lines in symbiotic stars and confirmed high polarization in the λλ6825, 7082 lines of RR Tel (Schmid & Schild 1994). Polarization is the strongest evidence to date supporting the Raman-effect hypothesis for their origin. In this paper, we present and discuss the first simultaneous observations of the O VI λλ1032, 1038 and λλ6825, 7082 lines in a symbiotic star.

2. THE HUT FAR-UV SPECTRUM

The Hopkins Ultraviolet Telescope (HUT) has been described by Davidsen et al. (1992). Updates and a preliminary review of the performance during the Astro-2 mission are covered in Kruk et al. (1995), so only brief details will be given here. HUT consists of a 0.9 m primary mirror that gathers light for a prime-focus, Rowland-circle spectrograph optimized for observations below 1200 Å. The point-source resolution is 2–4 Å, and the photon-counting detector samples the 820–1840 Å spectral range at ∼0.52 Å pixel^{-1} in first order. New coatings of silicon carbide on the primary mirror and spectrograph grating improved the overall throughput of HUT by more than a factor of 2 for Astro-2.

[1] Based on observations made with the Astro-2 observatory and the 3.9 m Anglo-Australian Telescope at Siding Spring.

[2] Department of Physics and Astronomy, Johns Hopkins University, Baltimore, MD 21218; espey@pha.jhu.edu.

[3] Department of Physics and Astronomy, University of Pittsburgh, Pittsburgh, PA 15260.

[4] Center for Astrophysics and Space Sciences, University of California, San Diego, La Jolla, CA 92093.

[5] Mount Stromlo and Siding Spring Observatories, Australian National University, Weston Creek Post Office, ACT 2611, Canberra, Australia.

[6] Department of Astronomy, University of Wisconsin—Madison, Madison, WI 53706.

TABLE 1

STRONGEST MEASURED LINES

LINE	FLUX (10^{-12} ergs cm^{-2} s^{-1})			MODEL RATIOS	
	Observed	Corrected[a]	Ratio[b]	Photoionization[c]	Collisional[d]
S VI$_{tot}$ λ937	6.8	36.5	9.0	0.2	31.0
He II λ958	2.0	9.6	2.4	...	...
C III λ977	2.5	10.5	2.6	2.2	4.8
N III λ991	5.5	21.8	5.4	0.3	15.7
Ne VI] λ1000	11.7	44.4	11.0	~0	0.4
O VI$_{tot}$ λ1035	387.4	1290.0	319.5	4.9	179.4
He II λ1085	17.4	49.6	12.3	...	...
Ne V]$_{tot}$ λ1134	12.7	31.6	7.8	0.2	5.2
S III/[Mg VI] λ1190	7.5	17.2	4.3	~0	...
[S V] λ1199	23.4	53.3	13.2	0.1	2.2
N V$_{tot}$ λ1240[e]	95.9	187.2	46.4	9.8	419.0
O V λ1371	5.9	11.5	2.8	...	88.0
Si IV$_{tot}$ λ1397	13.2	25.2	6.2	5.4	3.7
O IV]$_{tot}$ λ1402	41.1	82.9	20.5	2.7	495.8
N IV] λ1486	22.6	41.5	10.3	9.7	26.5
C IV$_{tot}$ λ1549	223.2	403.7	100.0	100.0	100.0
[Ne V] λ1575	9.4	17.0	4.2	0.2	...
[Ne IV] λ1602	5.5	9.8	2.4	0.9	...
He II λ1640	149.1	265.3	65.7	28.6	4.5
O III]$_{tot}$ λ1664	26.3	46.7	11.6	9.5	21.9
N III]$_{tot}$ λ1749	9.9	17.4	4.3	3.4	1.8
[Mg VI]/Si II λ1807	6.8	12.0	3.0	0.4	>0.03

[a] Extinction-corrected fluxes for $E(B-V) = 0.08$ (see § 3).
[b] Corrected line ratio relative to C IV = 100.
[c] Photoionization-model output (see § 3).
[d] Collisional model interpolated from Landini & Monsignori Fossi 1990 with log $T_e = 5.3$.
[e] Line may be affected by reduced instrumental sensitivity.

We observed RR Tel with HUT on 1995 March 12.5 UT, during the 10th day of the Astro-2 mission. To ensure proper acquisition and centering of the target in the aperture during this orbital-daylight observation, we acquired RR Tel on the blank slit. We then accumulated a total of 1080 s on the target through the 20″ diameter circular aperture. The high intensity of the UV emission lines in RR Tel required us to stop down the telescope aperture to protect the microchannel-plate detector and to keep dead-time corrections to less than 5%. Using a partially open door state, ~750 cm^2 of the primary mirror were exposed, which limited count rates to less than 15 counts s^{-1} at the peaks of the brightest emission lines.

The HUT data are processed with a specially developed package of IRAF[7] tasks. We first subtract a uniform dark-count background and the broad base of grating-scattered geocoronal Lyα determined from airglow-free regions below the 912 Å Lyman limit, where there is no detectable source flux. Our flux calibration uses on-orbit observations and white dwarf–model atmospheres as described by Kruk et al. (1995). This preliminary calibration is estimated to be accurate to $\lesssim$5%, though uncertainties may be slightly higher for partial-door-state observations, such as this one. RR Tel is bright down to the Lyman limit and requires a small correction for second-order light in the 1824–1840 Å region. This correction is determined from the observed flux in the 912–920 Å range and a ratio of 0.23 for second- to first-order efficiency. The raw count spectra are used to derive Poisson statistical errors for each pixel, which we propagate through the data reduction process. The signal-to-noise ratio of the continuum in the final calibrated spectrum is generally $\gtrsim$10 per resolution element.

[7] The Image Reduction and Analysis Facility (IRAF) is distributed by the National Optical Astronomy Observatories, which are operated by the Association of Universities for Research in Astronomy, Inc. (AURA), under cooperative agreement with the National Science Foundation.

3. THE FAR-UV LINES

The HUT data were measured by use of the SPECFIT software, developed by Kriss (1994), and the fluxes of the strongest lines are presented in Table 1. Line widths are not quoted, as they are dominated by the instrumental resolution (see Kruk et al. 1995). Where necessary, fits to blended lines were performed by using line ratios fixed at values seen in *IUE* high-resolution data. The extinction-corrected values quoted in Table 1 assume the interstellar extinction curve of Cardelli, Clayton, & Mathis (1989) with $R_V = 3.1$. The extinction value of $E(B-V) = 0.08$ is based upon measurements of the [Ne V] λ1575/λ2973 lines (Jordan, Mürset, & Werner 1994).

RR Tel is classified as a symbiotic, or slow, nova. Following an outburst in 1944, it has been in decline. The evolution of the emission-line spectrum of RR Tel has paralleled that of other, classical novae, with lines of ever higher excitation appearing with time. From *IUE* spectra taken in 1992, Mürset & Nussbaumer (1994) diagnosed an electron temperature of (12–19) × 10^3 K and an electron density of 10^5–10^7 cm^{-3} for the circumbinary nebula and a blackbody temperature of 135,000–150,000 K for the hot star. Using the same modified Zanstra method as Mürset & Nussbaumer, we obtain a blackbody temperature estimate of 133,000 K from the equivalent width of the He II λ1640 line, though this temperature may be larger by ~10% if a non-LTE model is assumed (see Mürset et al. 1991).

From both Figure 1 and Table 1, it is readily apparent that the O VI doublet is the strongest emission feature in the far-UV spectrum, with a measured equivalent width of 730 Å.

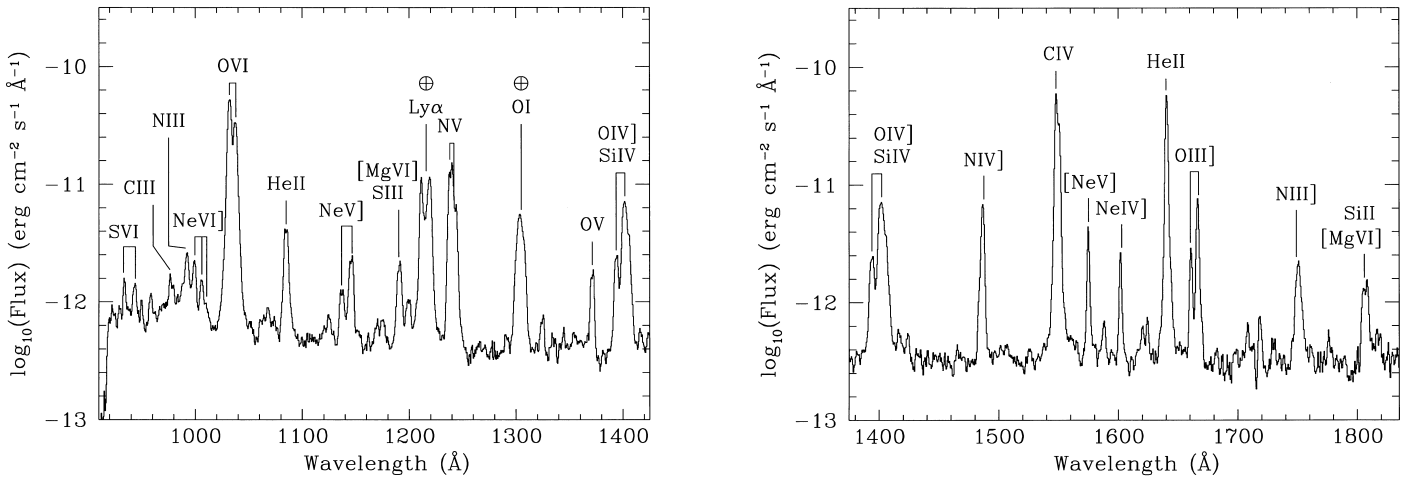

FIG. 1*a* FIG. 1*b*

FIG. 1.—HUT spectrum of RR Tel obtained during the Astro-2 mission, with the strongest emission lines marked. Airglow H I λ1216 and O I λ1304 emission are also indicated. Note that the spectrum is plotted on a logarithmic scale because of the high equivalent width of the strongest lines.

If we assume that O V λ1371 is predominantly produced by dielectronic recombination from O VI, then we can make an estimate of the temperature of the O VI region. Using the method of Nussbaumer & Storey (1984) together with the O VI collision strengths of Mendoza (1983), the predicted temperature of the O^{5+} region is $T_e \sim 2 \times 10^4$ K, which is consistent with the extinction-corrected value of O V λ1371/O V] λ1644 derived from *IUE* data (Doschek & Feibelman 1993). We also calculated nebular parameters using the HUT data for the Ne V] and Ne VI] lines that have ionization potentials bracketing that of O VI (Espey et al. 1995). The derived density and temperature are $n_e \sim 3 \times 10^6$ cm^{-3} and $T_e \sim 2 \times 10^4$ K, again consistent with other estimates (see, e.g., Hayes & Nussbaumer 1986).

The observed emission-line ratios along with the results of two simple models for comparison are given in Table 1. The photoionization model uses the CLOUDY code (Ferland 1993) to predict the spectrum of a constant-density cloud illuminated by the RR Tel ionizing spectrum (Jordan et al. 1994). Other parameters, including abundances, are similar to those of the model of Hayes & Nussbaumer (1986). The highest temperature in this model is similar to that derived from the diagnostics above, but the O VI doublet is weak. For comparison, a collisional model with solar abundances and a temperature ~1 order of magnitude larger is also shown. This model produces more O VI emission, but there are problems with other line ratios. It is apparent that a more complex model of the RR Tel system is necessary, but further discussions are deferred to a future paper.

4. SPECTROPOLARIMETRIC OBSERVATIONS OF THE RAMAN-SCATTERED O VI LINES

Spectropolarimetric observations of the Raman-scattered O VI λλ6825, 7082 emission lines in RR Tel were obtained with the 3.9 m Anglo-Australian Telescope (AAT) at Siding Spring during the night of 1995 March 8/9. The RGO spectrograph was set up as described by Hough & Bailey (1994). The 1200R grating and a 1024 × 1024 Tektronix CCD detector in the 25 cm camera yielded a wavelength coverage from 6400 to 7170 Å. The spectral resolution as measured from arc lines was 1.7 Å (FWHM), and the total exposure time for RR Tel was 44 minutes. Calibration was performed by observing the polarization standards HD 98161 and HD 298383 with the same instrumental setup. The data were reduced with a combination of the FIGARO software and special spectropolarimetric tasks from the TSP/Starlink package.

Figure 2 shows a part of the raw RR Tel spectrum together with the percentage polarization P and position angle θ. Strong polarization signals are visible for the Raman-scattered emission lines at λ6825 and λ7082. Both lines show a very similar polarization structure and sit on top of a continuum with a small, wavelength-independent polarization. We measure a mean continuum polarization and position angle of $P_c = 0.5\% \pm 0.1\%$ and $\theta_c = 169° \pm 6°$ over the wavelength range 6400–7200 Å, in excellent agreement with previous polarimetric observations by Schulte-Ladbeck & Magalhães (1987). Their measurements, together with the polarization map for surrounding stars (Schmid & Schild 1994), give ample

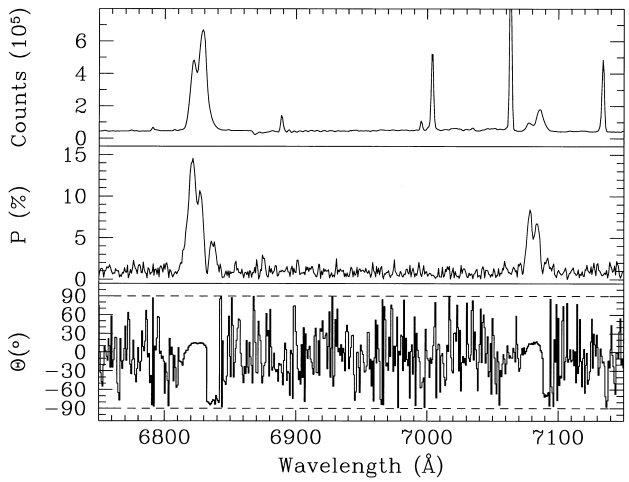

FIG. 2.—AAT spectropolarimetry of the Raman-scattered O VI lines in RR Tel. Shown are observed count spectrum (*top*), percentage polarization P (*middle*), and position angle θ (*bottom*). Each wavelength bin contains 1.5×10^5 counts. The errors in P, based on photon-counting statistics, are $\sigma_P = \pm 0.16\%$. The errors in θ scale approximately like σ_P/P and are therefore particularly large in the weakly polarized continuum.

evidence that the continuum polarization is predominantly due to interstellar dust grains. We therefore use the P_c and θ_c values to correct our data for interstellar polarization to obtain the intrinsic polarization structure in the Raman-scattered lines. Because of the small correction required to account for the effects of interstellar polarization, we do not include a separate figure, but the measurements that follow refer to the continuum-corrected data. There is no firm evidence for a variation in the mean polarization of the lines relative to lower resolution data taken in 1992 (Schmid & Schild 1994).

The Raman-scattered profiles consist of a main component with a weaker red component in each line, separated by a flip of ~90° in position angle. This is called a type III profile in the classification scheme of Schmid & Schild (1994), and they attributed the components to relative gas motions of the red giant's wind. Material traveling toward the hot star gives rise to a blueshifted Raman profile with a polarization vector perpendicular to the line that joins the two stars (the binary axis). For the λ6825 line, the flux-weighted mean position angle on the blue side of the flip is $\theta_{\rm blue} = 14\overset{\circ}{.}4$, and that on the red side is $\theta_{\rm red} = -83\overset{\circ}{.}8$ (or $96\overset{\circ}{.}2$). The corresponding angles for the λ7082 line are $\theta_{\rm blue} = 13\overset{\circ}{.}8$ and $\theta_{\rm red} = -76\overset{\circ}{.}8$ (or $103\overset{\circ}{.}2$). We can therefore deduce that the position angle of the binary components in RR Tel is $\theta = \theta_{\rm blue} + 90° = 104°$. In addition, the high overall scattering efficiency suggests that the plane of the binary system is close to the plane of the sky (Schmid 1992).

The atmospheric conditions during the AAT run precluded an accurate flux calibration, but because of the slow evolution of the RR Tel system, it is possible to calibrate the spectropolarimetry with auxiliary data taken close to the original observation date. Flux measurements were made under photometric conditions during the night of 1995 May 18/19 with the 74 inch (1.88 m) telescope at the Mount Stromlo Observatory. These data were reduced and flux-calibrated in a standard way, and the estimated overall flux accuracy is 15% for the stronger Raman-scattered line component and ~20% for the weaker. We adopt extinction-corrected line fluxes of 6.7×10^{-12} ergs s^{-1} cm^{-2} for the λ6825 line and 1.3×10^{-12} ergs s^{-1} cm^{-2} for the λ7082 line as representative of the fluxes during the Astro-2 mission.

The combined HUT and ground-based data enable us to calculate photon ratios of ~12 and ~36 for the O VI λ1032 line relative to the scattered features at λ6825 and λ7082, respectively. Because of the nearly plane-on nature of the binary, mentioned above, these measurements are representative of the O VI photon budget for the entire system. From the simulations of Schmid (1992) we thus estimate that 25%–50% of the emitted O VI photons must interact in the neutral scattering region. This in turn requires that the neutral region in RR Tel be very extended to cover such a large fraction of the O VI–emitting region. This is not unlikely, as the cool component of the system is a Mira variable with a spectral type later than M5 III (Feast & Glass 1974) that is losing ~10^{-6}–10^{-5} $M_\odot$ yr^{-1} (Kenyon, Fernández-Castro, & Stencel 1988; Seaquist & Taylor 1990).

Because of the extended nature of the scattering gas, it is highly likely that O VI photons that are moving away from the binary axis can also undergo Raman scattering. These photons will interact with gas, which has a significant recession velocity as viewed from the hot star, and thus the scattered photons become redshifted with a polarization closely parallel to the binary axis. The combination of blueshifted, perpendicularly polarized photons and redshifted, parallel polarized photons provides a convincing explanation for the observed polarization structure in the Raman lines. Although arguments have been raised against the Raman-scattering process in symbiotic systems (see, e.g., Kastner 1991), we consider that the balance of evidence presented here strongly favors this mechanism.

5. SUMMARY

From simultaneous far-UV spectra obtained with HUT on Astro-2 and AAT data, we deduce that Raman scattering of O VI emission occurs in RR Tel. The combination of strong O VI emission and an extended H I scattering region explains the strength of the scattered lines. The observed polarization structure is also well explained by the Raman process, and we deduce that the binary components lie along a position angle of $\theta = 104°$ and close to the plane of the sky. The accumulated UV and optical data provide more details on the properties of RR Tel, and these will be addressed in a future paper.

This work was supported by NASA contract NAS5-27000 to Johns Hopkins University. B. R. E. and R. S.-L. acknowledge financial support from Astro-2 Guest Investigator grants NAG8-1049 and NAG8-1073, respectively. H. M. S. is supported by a grant from the Swiss National Science Foundation. F. H. acknowledges support from NASA grant NAG5-1630.

REFERENCES

Allen, D. A. 1980, MNRAS, 190, 75
Cardelli, J. A., Clayton, G. C., & Mathis, J. S. 1989, ApJ, 345, 245
Davidsen, A. F., et al. 1992, ApJ, 392, 264
Doschek, G. A., & Feibelman, W. A. 1993, ApJS, 87, 331
Espey, B. R., Keenan, F., McKenna, F. C., Feibelman, W. A., & Aggarwal, K. M. 1995, ApJ, 454, L61
Feast, M. W., & Glass, I. S. 1974, MNRAS, 167, 81
Feibelman, W. A., Bruhweiler, F. C., & Johansson, S. 1991, ApJ, 373, 649
Ferland, G. J. 1993, Univ. Kentucky Phys. Dept. Internal Rep.
Hayes, M. A., & Nussbaumer, H. 1986, A&A, 161, 287
Hough, J. H., & Bailey, J. A. 1994, Spectropolarimetry at the AAT, AAO User Manual 24.2
Johansson, S. 1988, ApJ, 327, L85
Jordan, S., Mürset, U., & Werner, K. 1994, A&A, 283, 475
Kastner, S. O. 1991, Ap&SS, 185, 265
Kenyon S. J., Fernández-Castro, T., & Stencel, R. E. 1988, AJ, 95, 1817
Kriss, G. A. 1994, in ASP Conf. Proc. 61, Astronomical Data Analysis Software and Systems III, ed. D. R. Crabtree, R. J. Hanisch, & J. V. Barnes (San Francisco: ASP), 437
Kruk, J. W., Durrance, S. T., Kriss, G. A., Davidsen, A. F., Blair, W. P., Espey, B. R., & Finley, D. 1995, ApJ, 454, L1
Landini, M., & Monsignori Fossi, B. C. 1990, A&AS, 82, 229
Mendoza, C. 1983, in IAU Symp. 103, Planetary Nebulae, ed. D. R. Flower (Dordrecht: Reidel), 143
Mürset, U., & Nussbaumer, H. 1994, A&A, 587, 604
Mürset, U., Nussbaumer, H., Schmid, H. M., & Vogel, M. 1991, A&A, 248, 458
Nussbaumer, H., Schmid, H. M., & Vogel, M. 1989, A&A, 211, L27
Nussbaumer, H., & Storey, P. J. 1984, A&AS, 56, 293
Schmid, H. M. 1989, A&A, 211, L31
———. 1992, A&A, 254, 224
Schmid, H. M., & Schild, H. 1990, A&A, 236, L13
———. 1994, A&A, 281, 145
Schulte-Ladbeck, R. E., & Magalhães, A. M. 1987, A&A, 181, 213
Seaquist, E. R., & Taylor, A. R. 1990, ApJ, 349, 313